

Contribution of phases segregated from the UO_2 matrix to the release of radionuclides from spent nuclear fuel and duration of the Instant Release Fraction (IRF)

Alexandra Espriu-Gascon^a, Albert Martínez-Torrents^b, Daniel Serrano-Purroy^c, Javier Giménez^{a,*}, Joan de Pablo^{a,b}, Ignasi Casas^a

^a Departament d'Enginyeria Química, EEBE and Barcelona Research Center in Multiscale Science and Engineering, Universitat Politècnica de Catalunya, Eduard Maristany, 10-14, 08019, Barcelona, Catalonia, Spain

^b EURECAT, Centre Tecnològic de Catalunya, Plaça de la Ciència 2, 08243, Manresa, Barcelona, Spain

^c European Commission, DG Joint Research Centre, JRC, Directorate G, Nuclear Safety & Security, Department G.III, P.O. Box 2340, D-76125, Karlsruhe, Germany

ARTICLE INFO

Article history:

Received 8 October 2019

Received in revised form 14 February 2020

Accepted 15 February 2020

Available online xxx

Keywords

IRF

Spent nuclear fuel

Radionuclide

UO_2

ABSTRACT

During the dissolution of the spent nuclear fuel (SNF) some radionuclides are released to the solution simultaneously from different sources in the fuel. This is of particular importance to some radionuclides that contribute to the Instant Release Fraction (IRF), which govern the initial radiation dose during the dissolution of the SNF. In this work a model that is able to discriminate between the different contributions responsible for the total concentration of a radionuclide in solution was developed. The model permits to establish that uranium and radionuclides that dissolved congruently with the UO_2 matrix came from two sources as a function of time: oxidized phases on the surface of the SNF including fines and the matrix itself. Other radionuclides such as Ru and Rh were released from metallic precipitates with dissolution rates lower than the matrix dissolution rate. In the case of radionuclides that were expected to contribute to the IRF, this work showed that Cs, Rb and Sr had initial release rates higher than uranium because a fraction of such radionuclides were segregated from the matrix during the irradiation. Actually it was calculated that the fraction of those radionuclides in the grain boundaries in a BWR SNF powder sample from the center part of a pellet (burnup 42 MWd/kgU) was 2.1%, 0.9%, and 0.6% for Cs, Rb, and Sr, respectively. In addition, the model permitted to calculate the duration of their contribution to the IRF, matrix dissolution governed the release of such radionuclides after 137 days, 75 days, and 164 days for Cs, Rb, and Sr, respectively (at these times, the contribution of the release from grain boundaries was lower than the 0.1%).

© 2020

1. Introduction

In a Deep Geologic Repository (DGR) for spent nuclear fuel (SNF) it is assumed that the fuel will come into contact with water several thousand years after disposal, due to the use of massive metallic containers and other engineering barriers [1–4]. The dissolution of the SNF in contact with groundwater would result in the release of radionuclides and their migration through the geosphere. For the safety analysis of the DGR it is necessary to establish the mechanisms of radionuclides release as well as the dependence of the total release with time. In this sense, the FIRST-Nuclides Project [5–7] developed experimental and theoretical studies on the leaching of radionuclides from high-burnup SNF, which showed that fission products might be classified considering the ratio between their release rate and the UO_2 matrix dissolution rate. In particular, radionuclides with a release rate higher than

the matrix dissolution rate, the Instant Release Fraction (IRF) [8–10], are expected to govern the initial radiation dose at the beginning of the dissolution of the SNF [11]. The IRF might be also subdivided considering the localization of the radionuclides in the SNF [14–16]. On one hand, some radionuclides are segregated from the matrix and released to the gap region and to open grain boundaries that will be directly in contact with the water once the process of dissolution begins. This release is assumed to last for weeks or months [12]. On the other hand, some radionuclides segregated from the matrix are located in the grain boundaries. In this case, the dissolution is slower [12,13]. In both cases, it should not be forgotten that the radionuclides contributing to the IRF are also in the UO_2 matrix as well as in oxidized uranium phases that could have been formed on the surface of the SNF during its handling before the introduction in the reactor. Consequently, at the start of the SNF dissolution, radionuclides from the IRF are being released simultaneously from different sources.

Some SNF leaching experiments aimed to establish the different contributions to the IRF and their duration. However, the results obtained and their discussion by different authors showed that there is not a general agreement on the duration of each contribution. For ex-

* Corresponding author.

E-mail address: francisco.javier.gimenez@upc.edu (J. Giménez)

ample, some authors indicated that the release of radionuclides from the grain boundaries was not negligible after 200 days [11] while other authors determined that the release of the IRF for powdered SNF samples lasted 10 days [8]. As it was indicated by some authors [11,12], the uncertainties on the duration of the IRF release do not allow the accurate determination of the amount of each radionuclide released and segregated from the uranium matrix. Actually, it is complicated to determine the composition and duration of the IRF only from experimental data, because the experiments usually measure the total concentration of a radionuclide leached from the SNF, but such concentrations are not the consequence of the release of the radionuclide from a single source.

In the present work, a model based on experimental SNF leaching data was developed in order to determine the relative importance of the contribution from different sources on the total release of a radionuclide. The main objective was to determine how much radionuclide was released to the solution from each source in the SNF, and, consequently, what is the actual contribution of each radionuclide to the IRF and what is its duration.

2. Description of the mathematical model

The model, named Segregated Radionuclide Identification and Quantification Model (SERNIM), was based on two assumptions:

- 1) The total concentration of a radionuclide measured in the leaching solution is the sum of the radionuclide concentrations, which come from all the sources in the SNF. The model does not take into account any secondary phase precipitation after the dissolution process. For this reason, it will be fitted to experimental data obtained in experiments designed to avoid precipitation [11]. The experimental data used in this work [7] were obtained from the leaching of a BWR SNF powder sample from the center part of a pellet with 42 MWd/kgU of burn-up. The SNF sample was irradiated with an average linear power density and a maximum linear power density of 217 W cm⁻¹ and 293 W cm⁻¹, respectively. The fuel enrichment was 3.7% ²³⁵U and the fission gas release 2.3 ± 0.2% [7]. The experiments were performed under oxidizing conditions and introducing the fuel sample on a glass tube together with 50 mL of the leaching solution (1 mM HCO₃⁻). Samples were extracted at different times and the volume of sample was substituted by fresh leaching solution, the quantity of each radionuclide contained in the samples was taken into account in the cumulative moles of radionuclide released from the fuel. The concentration of the radionuclides in the solutions was determined by ICP-MS.
- 2) The release of the radionuclide from each source follows a first order kinetics.

The mathematical expression deduced from these assumptions is shown in Eq. (1).

$$m_{RN}(t) = \sum_c m(c)_{RN,t=\infty} \cdot (1 - e^{-k_c t}) \quad (1)$$

Where 'm_{RN}(t)' is the amount of radionuclide measured in the solution as a function of time (in moles) and 'm(c)_{RN,t=∞}' is the total moles of radionuclide released from contribution 'c' at infinite time. c denotes the source of the radionuclide leached: 'ma' matrix, 'ox' pre-oxidized uranium phases or fines, and 'seg' grain boundaries and gap (seg). 'k_c' is the kinetic dissolution constant of the 'c' contribution (in days⁻¹), and 't' is time (in days).

3. Results

3.1. Uranium release

Regarding the origin of the experimental data, in the case of uranium two different contributions were considered. One contribution was related to the uranium released from uranium-oxidized phases or fines (contribution 'ox') present on the surface of the SNF at the start of the experiment. The second contribution was related to the uranium released from the non-oxidized uranium matrix (contribution 'ma'). Considering both contributions, eq. (2) is deduced from eq. (1):

$$m_U(t) = m(ox)_{U,\infty} \cdot (1 - e^{-k_{ox}t}) + m(ma)_{U,\infty} \cdot (1 - e^{-k_{ma}t}) \quad (2)$$

SERNIM assumes that the parameter m(ma)_{U,∞} (moles of uranium in the matrix) is related to m(ox)_{U,∞} (moles of pre-oxidized uranium or uranium in fines) and the total uranium in the sample, which in turn is calculated considering the sample weight and the inventory of uranium in the SNF, according to eq. (3):

$$m(ma)_{U,\infty} = m_{U,TOTAL} - m(ox)_{U,\infty} = \frac{M_{sample} \cdot H_U}{MW} - m(ox)_{U,\infty} \quad (3)$$

Where 'm_{U,TOTAL}' is the total amount of uranium in the sample (in moles), 'M_{sample}' is the sample weight, 'H_U' is the uranium inventory in grams of uranium/grams of sample and 'MW' is the atomic weight of uranium. The inventory of uranium and of the other radionuclides in the fuel samples studied in this work was also experimentally determined by Martínez-Torrents et al. [7]. The authors dissolved the fuel powder with a mixture of HF and HNO₃ in a Parr Teflon bomb at 210 °C (an additional dissolution of the sample in HNO₃-HCl was carried out in order to correct the lanthanide fluoride precipitation). The solutions obtained (without any trace of solids) were analyzed by ICP-MS and γ-spectrometry [7].

The model was fitted to the experimental uranium released as a function of time by using Matlab® software. The specific mathematical tool was the "Curve Fitting Tool" which is based on the least square fitting routine. The parameters obtained by the fitting are shown in Table 1 while the comparison between the model and the experimental data can be seen in Fig. 1.

The dissolution rate corresponding to each contribution was calculated from the derivate of the general equation of the model as a function of time and normalized by the specific surface area (S = 4652 ± 2000 mm²) of the sample [7] (Eq. (4)).

$$r = \frac{dm_{RN}(t)}{S \cdot dt} = \frac{1}{S} \sum_c m(c)_{RN,\infty} \cdot k_c \cdot (e^{-k_c t}) \quad (4)$$

The dissolution rate of the matrix, 2.7·10⁻¹¹ mol m⁻² s⁻¹, is in good agreement with the release rate determined previously for the matrix dissolution by the Matrix Alteration Model (MAM) in the SFS project [15]: 4.6·10⁻¹¹ mol m⁻² s⁻¹, and very similar to the dissolution rate value determined experimentally within the SFS pro-

Table 1

Results of the fitting routine to the uranium leaching data in order to determine the parameters of the SERNIM.

Parameter	Value	Error	Units	Molar percentage (%)
m(ox) _{U,∞}	1.10 · 10 ⁻⁵	± 0.01 · 10 ⁻⁵	moles	3
k _{ox}	0.06	± 10 ⁻⁵	days ⁻¹	
m(ma) _{U,∞}	3.73 · 10 ⁻⁴	± 0.01 · 10 ⁻⁴	moles	97
k _{ma}	3.0 · 10 ⁻⁵	± 0.3 · 10 ⁻⁵	days ⁻¹	
R ²	0.95			

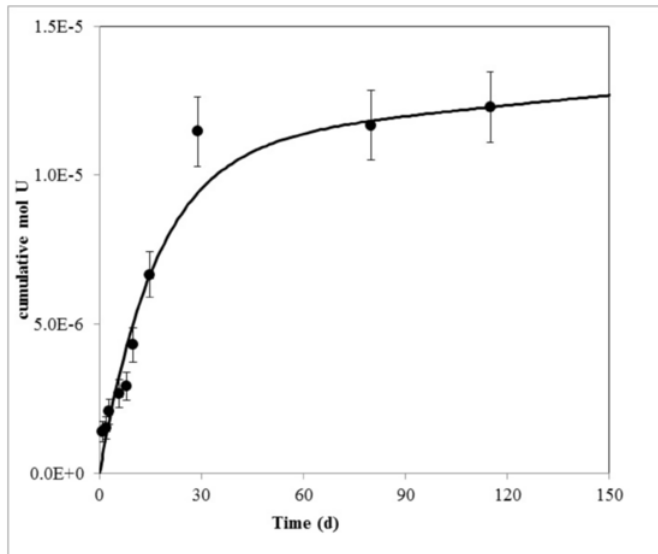


Fig. 1. Fitting of the uranium cumulative moles released from SNF with time. The continuous line represents the fitting of the SERNIM model ($R^2 = 0.95$) and the points represent the experimental values [7].

ject, $3.2 \cdot 10^{-11} \text{ mol m}^{-2} \text{ s}^{-1}$. In both cases, the composition of the leachate was the same than in the experimental values used to fit the SERNIM.

On the other hand, the dissolution rate of the oxidized phase, $1.6 \cdot 10^{-9} \text{ mol m}^{-2} \text{ s}^{-1}$, is found to be two orders of magnitude higher than the matrix dissolution rate. A higher dissolution rate was not surprising because of the known higher dissolution rate of the uranium oxidized phases, in particular in the presence of bicarbonate, which forms very stable complexes with U(VI) [16–19]. Additionally, the results obtained coincide with the rates determined by Gray and Wilson [20] who observed an increase of two orders of magnitude on dissolution rates when comparing the dissolution of oxidized and non-oxidized fuel.

Focusing on the development on the model, the coincidence between the calculated and the previously determined uranium dissolution rates reinforces the assumptions made in the model and its robustness.

3.2. Radionuclides release

Regarding the release of other radionuclides, if they are homogeneously dissolved in the uranium matrix, their release, corrected con-

sidering the inventory of each radionuclide, should be the same than uranium. In other words, if the release behavior is different from uranium, the release of the radionuclide should be due not only to the dissolution of oxidized phases and matrix but to the dissolution of phases segregated from the matrix. In order to determine the behavior of the radionuclides release compared to that of uranium, the model was fitted using the values of the kinetic constants k_{ox} and k_{ma} determined for uranium and, for each fitting, eq. (3) was used considering for each radionuclide its atomic weight and its inventory. The inventory was considered to be constant during the experimental time.

From the fitting of the model to different radionuclides, two different behaviors were observed. For some radionuclides, the model fitted the experimental data with the kinetic constants determined for uranium and taking into account the inventory of the radionuclide (such radionuclides will be congruently released with the UO_2 matrix). On the other hand, other radionuclides were released faster or slower than uranium, and the model was not able to fit the experimental data only considering kinetic constants for uranium and inventory (radionuclides that will be not congruently released with the UO_2 matrix).

3.2.1. Radionuclides with a release behavior similar to uranium (congruently released with the UO_2 matrix)

The elements whose dissolution was well predicted by using the parameters deduced for uranium (and considering their inventory) were Tc, Mo, Am, Pu, Ce and La (see Table 2).

As an example, the release of cerium was predicted by using the parameters determined by the uranium release corrected by the inventory ($H_{\text{Ce}} = 2663 \mu\text{gCe}\cdot\text{g}^{-1}$). The parameters obtained for the processes of release from the oxidized phases and matrix were $m(\text{ox})_{\text{Ce},\infty} = (6.0 \pm 0.7) \cdot 10^{-8} \text{ mol}$ and $m(\text{ma})_{\text{Ce},\infty} = (2.03 \pm 0.01) \cdot 10^{-6} \text{ mol}$ (see Table 2). The fitting of the model to the experimental data with those parameters ($R^2 = 0.95$) is shown in Fig. 2, where it can be seen that the cerium release obtained with the SERNIM is in good agreement with the experimental release data.

The actinides Pu and Am and the lanthanides La and Ce were expected to be congruently released with the matrix, because previous works pointed to their homogeneous dissolution in the matrix [8,11,21]. On the other hand, under the conditions of the experiments used in this work for the development of the mathematical model, technetium and molybdenum were congruently released with the UO_2 matrix. This behavior was surprising, because they were expected to be contained in the metallic inclusions, while Mo could be partially dissolved as oxide in the fuel matrix. Their release from metallic inclusions could result in a non-congruent dissolution with the matrix, as it is observed, for example, in the recent preliminary experiments car-

Table 2

Values of the $m(\text{c})$ (moles) and (%) and k_{c} parameter obtained by the algorithm for 12 radionuclides from leaching data of a 42 BWR CORE sample.

RN	$m(\text{seg})$	$m(\text{ox,U})$	$m(\text{ma})$	$m(\text{seg})(\%)$ (± 0.1)	$m(\text{ox,U})(\%)$ (± 0.1)	$m(\text{ma})(\%)$ (± 0.1)	k_{seg}	$k_{\text{ox}} (\pm 10^{-5})$	$k_{\text{ma}} (\pm 3 \cdot 10^{-6})$
U		$1.10 \cdot 10^{-5}$	$3.73 \cdot 10^{-4}$		2.9%	97.1%		0.06	$2.96 \cdot 10^{-5}$
Cs	$4.63 \cdot 10^{-8}$	$6.5 \cdot 10^{-8}$	$2.14 \cdot 10^{-6}$	2.1%	2.9%	95.1%	0.08	0.06	$2.96 \cdot 10^{-5}$
Sr	$8.71 \cdot 10^{-9}$	$3.8 \cdot 10^{-8}$	$1.29 \cdot 10^{-6}$	0.6%	2.9%	96.5%	0.13	0.06	$2.96 \cdot 10^{-5}$
Tc		$2.7 \cdot 10^{-8}$	$9.02 \cdot 10^{-7}$		2.9%	97.1%		0.06	$2.96 \cdot 10^{-5}$
Mo		$1.2 \cdot 10^{-7}$	$4.10 \cdot 10^{-6}$		2.9%	97.1%		0.06	$2.96 \cdot 10^{-5}$
Rb	$5.05 \cdot 10^{-9}$	$1.6 \cdot 10^{-8}$	$5.35 \cdot 10^{-7}$	0.9%	2.9%	96.2%	0.06	0.06	$2.96 \cdot 10^{-5}$
Am		$2.8 \cdot 10^{-9}$	$9.45 \cdot 10^{-8}$		2.9%	97.1%		0.06	$2.96 \cdot 10^{-5}$
Rh ^a		$1.4 \cdot 10^{-8}$	$4.87 \cdot 10^{-7}$		2.9%	97.1%		0.06	$2.96 \cdot 10^{-5}$
Ru ^a		$7.5 \cdot 10^{-8}$	$2.54 \cdot 10^{-6}$		2.9%	97.1%		0.06	$2.96 \cdot 10^{-5}$
Pu		$1.3 \cdot 10^{-7}$	$4.51 \cdot 10^{-6}$		2.9%	97.1%		0.06	$2.96 \cdot 10^{-5}$
Ce		$6.0 \cdot 10^{-8}$	$2.03 \cdot 10^{-6}$		2.9%	97.1%		0.06	$2.96 \cdot 10^{-5}$
La		$3.3 \cdot 10^{-8}$	$1.13 \cdot 10^{-6}$		2.9%	97.1%		0.06	$2.96 \cdot 10^{-5}$

^a Elements that were over estimated by SERNIM by using the parameters values shown in the table.

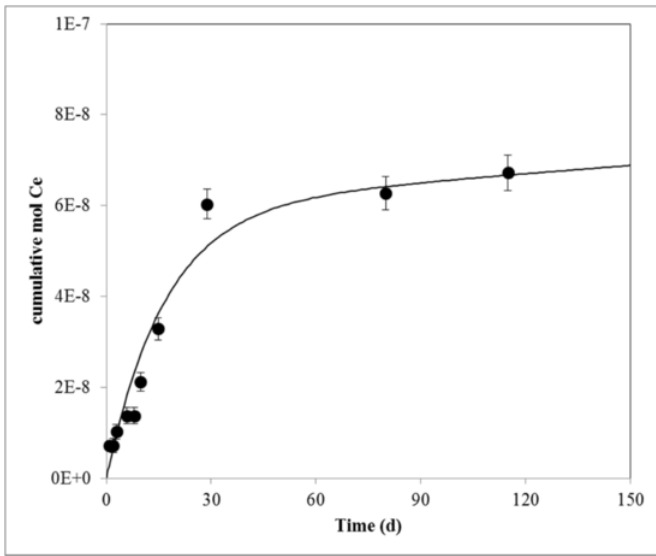


Fig. 2. Fitting of the cerium cumulative moles released from SNF with time. The continuous line represents the fitting of the SERNIM model ($R^2 = 0.95$) and the points represent the experimental results [7].

ried out in the frame of the DisCo European project [22]. Considering only the data obtained in this work, due to of the technetium and molybdenum congruent dissolution with the UO_2 matrix, they would not contribute to the IRF.

3.2.2. Radionuclides with experimental dissolution rates lower than predicted by the SERNIM

When the release behavior of a radionuclide was different from uranium, the release calculated with the SERNIM could be lower or higher than the experimental release depending on the source and chemical form of the radionuclide in the fuel.

If the experimental release of a radionuclide was lower than the release predicted by the SERNIM, the radionuclide was supposed to be forming a solid phase less soluble than the matrix. This was the case for Ru and Rh. For example, the parameters obtained for the process of ruthenium release from the oxidized phases and matrix were $m(\text{ox})_{\text{Ru},\infty} = (7.5 \pm 0.9) \cdot 10^{-8}$ mol and $m(\text{ma})_{\text{Ru},\infty} = (2.54 \pm 0.01) \cdot 10^{-6}$ mol (using an inventory of $H_{\text{Ru}} = 2407.9 \mu\text{gRu}\cdot\text{g}^{-1}$). By using these values on the fitting, the predicted release of ruthenium was much higher than the experimental release data (see Fig. 3).

The behavior of Ru and Rh was not surprising since they are believed to be on the SNF as metallic precipitates particles. These particles were reported in previous works [23–25] and, recently, Mennecart et al. [26] observed a metallic alloy precipitate containing Ru and Rh in a SNF sample with an average BU of 50.5 MWd/kgU. The presence of these radionuclides in solid phases with different dissolution rates from uranium dioxide would explain the discrepancy between calculated and experimental values. In this case, the parameters fixed considering the dissolution of uranium would not be appropriate, because Ru and Rh would be releasing from another solid phase with a different dissolution rate than uranium. In any case, due to their lower release rate, Ru and Rh are not considered to contribute to the IRF.

3.2.3. Radionuclides with experimental dissolution rates higher than the predicted by the SERNIM

A third group of radionuclides showed experimental dissolution rates higher than the predicted by the SERNIM with the mechanisms assumed to govern the release of uranium. In this work, three radionuclides were found to be integrated in this group: Cs, Sr and Rb.

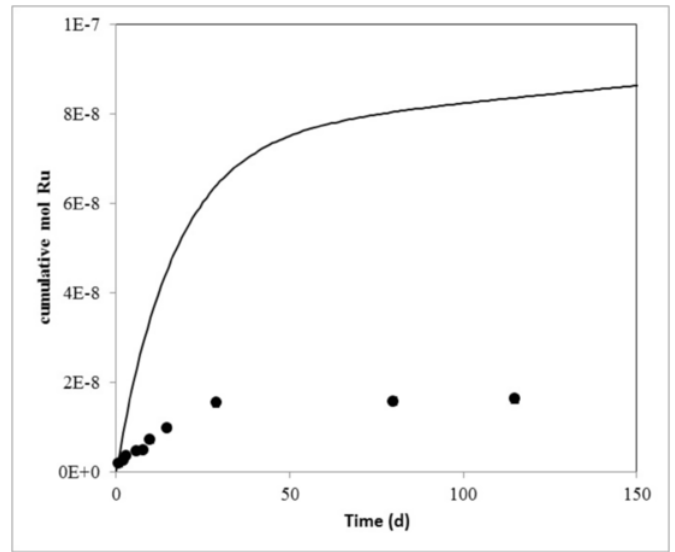


Fig. 3. Fitting of the ruthenium cumulative moles released from SNF with time. The continuous line represents the fitting of the SERNIM model, the points represent the experimental results [7].

For example, SERNIM was used in order to fit the release of cesium considering its release only from oxidized phases or fines and from the matrix. Considering the inventory of cesium ($H_{\text{Cs}} = 2727.2 \mu\text{gCs}\cdot\text{g}^{-1}$), the parameters obtained for the processes of release from the oxidized phases and matrix were $m(\text{ox})_{\text{Cs},\infty} = (6.5 \pm 0.8) \cdot 10^{-8}$ mol and $m(\text{ma})_{\text{Cs},\infty} = (2.14 \pm 0.01) \cdot 10^{-6}$ mol. As it can be seen in Fig. 4, the model could not fit the experimental values.

If it is assumed that the higher cesium release is a consequence of the presence of cesium segregated from the matrix, a new contribution should be included in the model, accounting for the cesium released from such source. In this sense, an additional term accounting for cesium segregated from the matrix was added and the SERNIM was expressed as in Eq. (5):

$$m_{\text{Cs}}(t) = m(\text{seg})_{\text{Cs},\infty} \cdot (1 - e^{-k_{\text{seg}}t}) + m(\text{ox}, U)_{\text{Cs},\infty} \cdot (1 - e^{-k_{\text{ox}}t}) + m(\text{ma})_{\text{Cs},\infty} \cdot e^{-k_{\text{mat}}t}$$

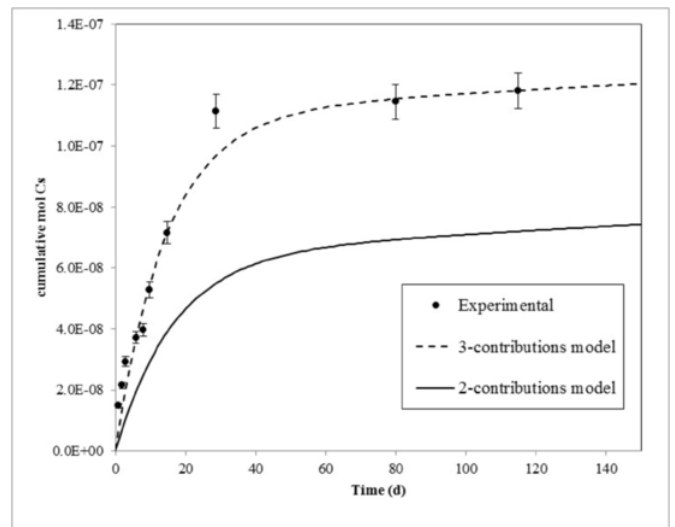


Fig. 4. Fitting of the cesium cumulative moles released from SNF with time. The points represent the experimental results [7].

The actual meaning of this additional term would be related to cesium located neither in the matrix nor in the oxidized uranium phases or fines, but in the grain boundaries and in the gap. However, in the experiments used in this work [7] the gap contribution could be neglected because the experiments were carried out with crushed solid from the central part of the fuel. Hence, in this case, the additional release mechanism for Cs (and for Rb and Sr) accounts only for the radionuclide segregated in the grain boundaries.

The term added to SERNIM introduced two more parameters: $m(seg)_{Cs,\infty}$ is the amount of moles released by cesium segregated in the grain boundaries, and k_{seg} is the kinetic constant for the dissolution of the segregated phase. The parameter ' $m(ma)_{Cs,\infty}$ ' was adjusted to accomplish with the mass balance as it is shown in Eq. (6):

$$m(ma)_{Cs,\infty} = m_{Cs,TOTAL} - m(seg)_{Cs,\infty} - m(ox,U)_{Cs,\infty} = \frac{M_{sample} \cdot H_{Cs}}{MW} - m(s$$

Thus, $m(ox,U)$, k_{ox} and k_{ma} were fixed to the values reported for uranium while $m(seg)_{Cs,\infty}$, k_{seg} and $m(ma)_{Cs,\infty}$ were determined by fitting of the experimental data with the model. The parameters obtained are shown in Table 3 and the fitting of the three-contributions SERNIM to the experimental data can be seen in Fig. 4. By using the parameters obtained from the SERNIM, it was determined that the 2.1% (± 0.1) of Cs is located at the grain boundaries. This result is in good agreement with the reported distribution of Cs in the SNF and with the percentage of Cs at the grain boundaries determined in previous experiments [7,25]. The moles of cesium released from each contribution are shown in Fig. 5.

From the fitting of the model with the three contributions to the experimental results of rubidium and strontium, it was calculated that the amount of Rb and Sr segregated at the grain boundaries was 0.9% and 0.6% ($\pm 0.1\%$), respectively. These values agree with previously reported values for rubidium [7,8] and strontium [7,8,25,27].

Due to their higher release during the first days of the leaching, Cs, Sr, and Rb should be considered to contribute to the IRF. One of the objectives of the development of the SERNIM was to establish the duration of the IRF, which might be determined from the kinetic parameters obtained after the fitting of the model to the experimental data. One of the advantages of the SERNIM is the possibility to discriminate between the different sources that contribute to the total concentration of the radionuclide in solution. In this sense, it was possible to calculate the percentage of cesium released from each contribution as a function of time, as it is shown in Fig. 6. As it can be seen, at the start of the process of leaching, the dissolution of the oxidized phases and the release of cesium in the grain boundaries predominated. Over time, the matrix dissolution became the predominant process of releasing cesium and the other two contributions fade over time. From Fig. 6, it was also possible to determine the end of the contribution of cesium to the IRF; at 120 days, the contribution is very low and, actually, the per-

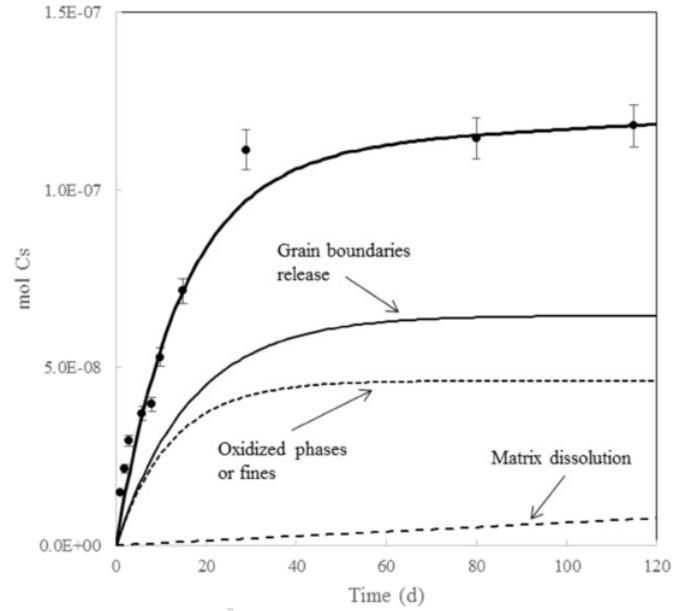


Fig. 5. Moles of cesium released with time from the different contributions according to the model.

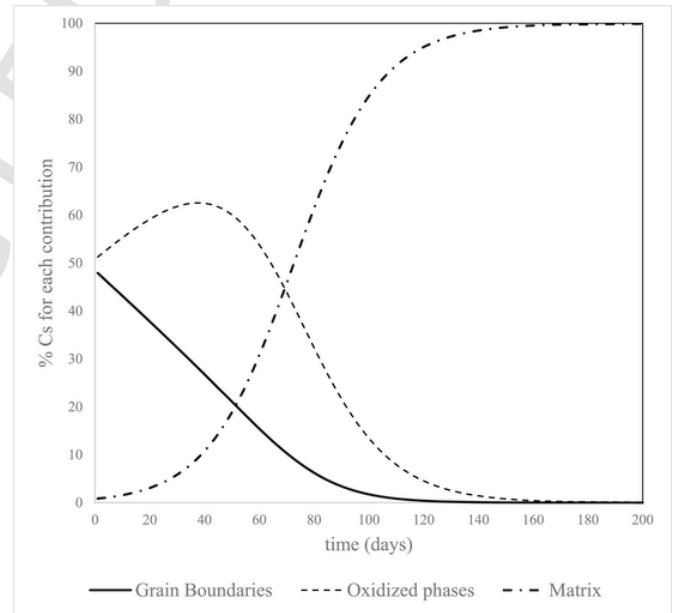


Fig. 6. Percentage of cesium released from the three contributions as a function of time.

centage of cesium released from that source is lower than the 0.1% after 137 days.

The same calculations were made with the data from rubidium and strontium (see Figs. 7 and 8). Fig. 9 shows for cesium, strontium and rubidium only the percentage of radionuclide released from grain boundaries as a function of time. For strontium and rubidium, the time at which percentages released are lower than 0.1% were calculated to be 75 days and 164 days, respectively.

4. Conclusions

The model developed in this work was able to fit the variation of the concentration of uranium and radionuclides congruently released with the matrix in SNF leaching experiments. In addition, uranium release rates obtained from the model are in agreement with dissolution rates previously reported.

Table 3

Values of the SERNIM parameters to adjust the SERNIM to the experimental release data of Cs.

Parameter	Value	Error	Units	Molar percentage (%)
$m(seg)_{Cs,\infty}$	$5 \cdot 10^{-8}$	$\pm 1 \cdot 10^{-8}$	moles	2.06
k_{seg}	0.08	± 0.06	days ⁻¹	
$m(ox,U)_{Cs,\infty}$	$6.5 \cdot 10^{-8}$	$\pm 0.8 \cdot 10^{-8}$	moles	2.87
k_{ox}	$6.0 \cdot 10^{-2}$	$\pm 10^{-5}$	days ⁻¹	
$m(ma)_{Cs,\infty}$	$2.14 \cdot 10^{-6}$	$\pm 0.02 \cdot 10^{-6}$	moles	95.07
k_{ma}	$3.0 \cdot 10^{-5}$	$\pm 0.3 \cdot 10^{-5}$	days ⁻¹	
R^2	0.96			

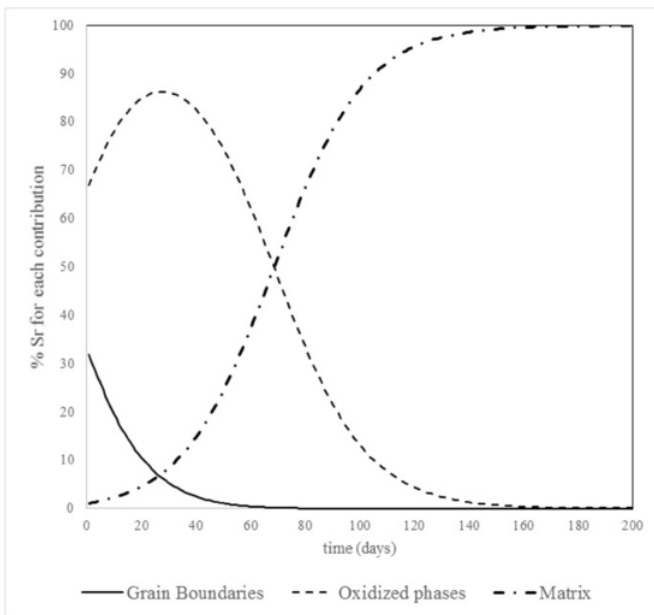


Fig. 7. Percentage of strontium released from the three contributions as a function of time.

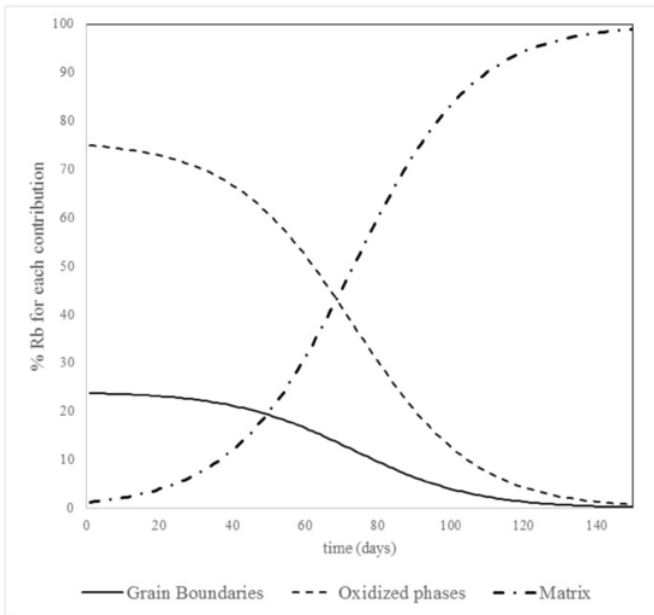


Fig. 8. Percentage of rubidium released from the three contributions as a function of time.

The fitting of the model to experimental data from Mo, Tc, Pu, Am, Ce and La showed that such radionuclides dissolve congruently with the matrix during the experimental time. Their concentration in solution was predicted by considering two contributions: (1) dissolution from oxidized phases or fines located on the SNF, and (2) dissolution of the matrix. On the other hand, the model could not fit the concentrations of Ru and Rh in solution considering only those two contributions, indicating that these radionuclides were segregated from the matrix, as it was expected because in the SNF they are believed to be in the form of metallic precipitates, with dissolution rates lower than the matrix. Radionuclides released congruently with uranium and radionuclides with dissolution rates lower than the matrix dissolution rate are not expected to contribute to IRF.

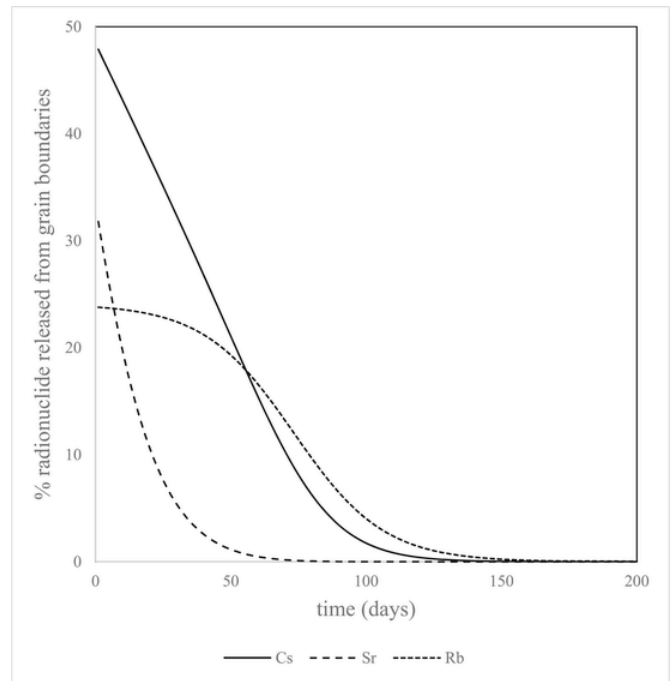


Fig. 9. Percentage of radionuclides released from the grain boundaries as a function of time.

For radionuclides with dissolution rates higher than the matrix (Cs, Rb and Sr), the model was applied including an additional contribution that considered the fraction of radionuclide that was segregated from the matrix to the grain boundaries, by adding this contribution, the model was adequately fitted to the experimental data. The fraction of the radionuclide segregated to grain boundaries was calculated to be 2.1%, 0.9%, and 0.6% for Cs, Rb, and Sr, respectively ($\pm 0.1\%$).

The ability of the model to discriminate between the different sources of radionuclide release to the solution permitted to determine that the contribution of the release of the radionuclide from grain boundaries was decreasing with time and was lower than the 0.1% at 137 days, 75 days, and 164 days for Cs, Sr, and Rb, respectively.

Disclaimer

This presentation only expresses the opinion of the authors and neither ACCÍO nor the European Union is responsible of the use of the given information.

CRediT authorship contribution statement

Alexandra Espriu-Gascon: Formal analysis, Investigation, Writing - original draft. **Albert Martínez-Torrents:** Conceptualization, Validation, Resources. **Daniel Serrano-Purroy:** Validation, Resources, Supervision. **Javier Giménez:** Validation, Writing - original draft, Writing - review & editing. **Joan de Pablo:** Conceptualization, Methodology, Writing - review & editing, Funding acquisition. **Ignasi Casas:** Conceptualization, Methodology, Writing - review & editing, Funding acquisition.

Declaration of competing interest

The authors declare that they have no known competing financial interests or personal relationships that could have appeared to influence the work reported in this paper.

Acknowledgments

The research leading to these results has received funding from: (1) ENRESA, under ENRESA/ITU/CTM 31698 Agreement. (2) The program People (Marie Curie Actions), 7th Framework Programme from the European Union (FP7/2007–2013) under the agreement n600388 from REA. (3) The Agency for Business Competitiveness (ACCIO). (4) The European Union's European Atomic Energy Community's (Euratom) Seventh Framework Programme FP7/2007–2011 under grant agreement n° 295722 (FIRST-Nuclides project). (5) The Ministerio de Economía y Competitividad (Spain) with the project ENE2017-83048-R. A. Espriu Gascon thanks to Ministerio de Economía y Competitividad (Spain) for her fellowship BES-2012-053098.

References

- [1] C.N. Wilson, Results from NNWSI [Nevada Nuclear Waste Storage Investigations] Series 2 Bare Fuel Dissolution Tests, Richland, Washington, USA, 1990.
- [2] D.W. Shoesmith, Fuel corrosion processes under waste disposal conditions, *J. Nucl. Mater.* 282 (2000) 1–31.
- [3] J. Bruno, R.C. Ewing, Spent nuclear fuel, *Elements* 2 (2006) 343–349.
- [4] R.C. Ewing, Long-term storage of spent nuclear fuel, *Nat. Mater.* 14 (2015) 252–257.
- [5] B. Kienzler, L. Duro, K. Lemmens, V. Metz, J. de Pablo, A. Valls, D.H. Wegen, L. Johnson, K. Spahiu, Summary of the Euratom collaborative project FIRST-nuclides and conclusions for the safety case, *Nucl. Technol.* 198 (2017) 260–276.
- [6] K. Lemmens, E. González-Robles, B. Kienzler, et al., Instant release of fission products in leaching experiments with high burn-up nuclear fuels in the framework of the Euratom project FIRST- Nuclides, *J. Nucl. Mater.* 484 (2017) 307–323.
- [7] A. Martínez-Torrents, D. Serrano-Purroy, R. Sureda, et al., Instant release fraction corrosion studies of commercial UO₂ BWR spent nuclear fuel, *J. Nucl. Mater.* 488 (2017) 302–313.
- [8] D. Serrano-Purroy, F. Clarens, E. González-Robles, et al., Instant release fraction and matrix release of high burn-up UO₂ spent nuclear fuel: effect of high burn-up structure and leaching solution composition, *J. Nucl. Mater.* 427 (2012) 249–258.
- [9] L. Johnson, C. Ferry, C. Poinssot, et al., Spent fuel radionuclide source-term model for assessing spent fuel performance in geological disposal. Part I: assessment of the instant release fraction, *J. Nucl. Mater.* 346 (2005) 56–65.
- [10] L. Johnson, C. Poinssot, C. Ferry, et al., Estimates of the Instant Release Fraction for UO₂ and MOX Fuel at T=0, NAGRA: Wettingen, Switzerland, 2004 Technical Report 04-08.
- [11] E. González-Robles, D. Serrano-Purroy, R. Sureda, et al., Dissolution experiments of commercial PWR (52 MWd/kgU) and BWR (53 MWd/kgU) spent nuclear fuel clad segments in bicarbonate water under oxidizing conditions. Experimental determination of matrix and instant release fraction, *J. Nucl. Mater.* 465 (2015) 63–70.
- [12] L. Johnson, I. Günther-Leopold, J. Kobler Waldis, et al., Rapid aqueous release of fission products from high burn-up LWR fuel: experimental results and correlations with fission gas release, *J. Nucl. Mater.* 420 (2012) 54–62.
- [13] L.O. Werme, L.H. Johnson, V.M. Oversby, et al., Spent Fuel Performance under Repository Conditions: A Model for Use in SR-Can, SKB, Stockholm, Sweden, 2004 Technical Report TR-04-19.
- [14] O. Roth, J. Low, M. Granfors, et al., Effects of matrix composition on instant release fractions from high burn-up nuclear fuel, *Mater. Res. Soc. Symp. Proc.*, Cambridge University Press, Boston, USA, 2013, pp. 145–150.
- [15] C. Poinssot, C. Ferry, M. Kelm, et al., Final Report of the European Project Spent Fuel Stability under Repository Conditions, European Commission Report CEA: France, 2005.
- [16] J. de Pablo, I. Casas, J. Giménez, et al., The oxidative dissolution mechanism of uranium dioxide. I. The effect of temperature in hydrogen carbonate medium, *Geochem. Cosmochim. Acta* 63 (1999) 3097–3103.
- [17] S. Röllin, K. Spahiu, U. Eklund, Determination of dissolution rates of spent fuel in carbonate solutions under different redox conditions with a flow-through experiment, *J. Nucl. Mater.* 297 (2001) 231–243.
- [18] J. Giménez, F. Clarens, I. Casas, et al., Oxidation and dissolution of UO₂ in bicarbonate media: implications for the spent nuclear fuel oxidative dissolution mechanism, *J. Nucl. Mater.* 345 (2005) 232–238.
- [19] B.T. Suzuki, A. Abdelouas, B. Grambow, et al., Oxidation and dissolution rates of UO₂(s) in carbonate-rich solutions, *Radiochim. Acta* 94 (2006) 567–573.
- [20] W.J. Gray, C.N. Wilson, Spent Fuel Dissolution Studies FY 1991 to 1994, Richland, Washington, USA, 1995.
- [21] V. Metz, H. Geckeis, E. González-Robles, A. Loida, C. Bube, B. Kienzler, Radionuclide behaviour in the near-field of a geological repository for spent nuclear fuel, *Radiochim. Acta* 100 (2012) 699–713.
- [22] M. Herm, E. González-Robles, L. Iglesias, P. Carbol, D. Serrano-Purroy, A. Barreiro, O. Roth, I. Casas, DISCO deliverable 3.1: spent fuel experiments: first dissolution results, *Ref. Ares* (2019) 4117760.
- [23] H. Kleykamp, The chemical state of the fission products in oxide fuels, *J. Nucl. Mater.* 131 (1985) 221–246.
- [24] D. Serrano-Purroy, F. Clarens, J.-P. Glatz, D.H. Wegen, B. Christiansen, J. de Pablo, J. Giménez, I. Casas, A. Martínez-Esparza, Leaching of 53 MW/d kg

U spent nuclear fuel in a flow-through reactor, *Radiochim. Acta* 97 (2009) 491–496.

- [25] D. Roudil, C. Jégou, V. Broudic, S. Muzeau, S. Peugot, X. Deschanel, Gap and grain boundaries inventories from pressurized water reactor spent fuels, *J. Nucl. Mater.* 362 (2007) 411–415.
- [26] T. Mennecart, K. Lemmens, C. Cachoir, Characterisation and leaching test for the experimental determination of IRF radionuclides from belgian high-burnup spent nuclear fuel, in: B. Kienzler, V. Metz, A. Valls (Eds.), Final Workshop Proceedings of the Collaborative Project “Fast/Instant Release of Safety Relevant Radionuclides from Spent Nuclear Fuel” (7th EC FP CP FIRST-Nuclides), KIT Scientific Publishing, Karlsruhe, Germany, 2014, pp. 147–156.
- [27] D. Roudil, C. Jégou, V. Broudic, M. Tribet, Rim instant release radionuclide inventory from French high burnup spent UOX fuel, *Mater. Res. Soc. Symp. Proc.* 1193 (2013) 145–150.